THE JOURNAL OF BIOLOGICAL CHEMISTRY VOL. 285, NO. 21, pp. 15816–15827, May 21, 2010

Mycobacterium tuberculosis Origin of Replication and the Promoter for Immunodominant Secreted Antigen 85B Are the Targets of MtrA, the Essential Response Regulator*[S]

Received for publication, July 2, 2009, and in revised form, March 10, 2010 Published, JBC Papers in Press, March 11, 2010, DOI 10.1074/jbc.M109.040097

Malini Rajagopalan[‡], Renata Dziedzic[‡], Maha Al Zayer[‡], Dorota Stankowska[‡], Marie-Claude Ouimet[§], D. Patrick Bastedo[§], Gregory T. Marczynski[§], and Murty V. Madiraju[‡1]

From [‡]Biomedical Research, University of Texas Health Science Center, Tyler, Texas 75708-3154 and the [§]Department of Microbiology and Immunology, McGill University, Montreal, Quebec H3A 2B4, Canada

Efficient proliferation of *Mycobacterium tuberculosis* (*Mtb*) inside macrophage requires that the essential response regulator MtrA be optimally phosphorylated. However, the genomic targets of MtrA have not been identified. We show by chromatin immunoprecipitation and DNase I footprinting that the chromosomal origin of replication, *ori*C, and the promoter for the major secreted immunodominant antigen Ag85B, encoded by *fbp*B, are MtrA targets. DNase I footprinting analysis revealed that MtrA recognizes two direct repeats of GTCACAgcg-like sequences and that MtrA∼P, the phosphorylated form of MtrA, binds preferentially to these targets. The *ori*C contains several MtrA motifs, and replacement of all motifs or of a single select motif with TATATA compromises the ability of *ori*C plasmids to maintain stable autonomous replication in wild type and MtrA-overproducing strains, indicating that the integrity of the MtrA motif is necessary for *ori*C replication. The expression of the *fbp*B gene is found to be down-regulated in *Mtb* cells upon infection when these cells overproduce wild type MtrA but not when they overproduce a nonphosphorylated MtrA, indicating that MtrA∼P regulates *fbp*B expression. We propose that MtrA is a regulator of *ori*C replication and that the ability of MtrA to affect apparently unrelated targets, *i.e.* *ori*C and *fbp*B, reflects its main role as a coordinator between the proliferative and pathogenic functions of *Mtb*.

Approximately one-third of the world population is latently infected with *Mycobacterium tuberculosis* (*Mtb*), the causative agent of tuberculosis. Studies with the mouse model of aerosol infection suggest that *Mtb* multiplication in the lung often continues uninterrupted until the mounting of host-adaptive immunity (reviewed in Ref. 1). This process results in pathogen growth arrest in the infected macrophages (MΦ)[2] and leads to the formation of granulomas. The bacteria in the granulomatous lesions are believed to be in a "latent or persistent state" and maintain a limited bacterial turnover but to resume active multiplication and cause infection when the host immune system is compromised (reviewed in Refs. 1–3). It is intriguing and largely unknown how *Mtb* multiplication is regulated upon infection or during survival in the persistent state. Mining the *Mtb* genome sequence data revealed that the pathogen operates a host of regulatory networks, including the paired two-component regulatory signal transduction systems (2CRS), several of which are believed to be required for virulence (4). The roles of several key players involved in these regulatory networks are largely unknown.

Paired 2CRS are the major means by which bacteria sense and respond to different stimuli and regulate gene expression through a phosphorylation relay (reviewed in Ref. 5). The *Mtb* genome encodes 11 paired 2CRS, among which MtrAB is the only essential 2CRS (4, 6, 7). This system consists of MtrB, a membrane-bound sensor kinase, which is nonessential for growth, and MtrA, a cytosolic response regulator (RR), which is essential, and knock-out strains of *mtr*A could not grow in broth unless a second copy of *mtrA* was present (7). The *mtr*A promoter activity is differentially expressed in virulent *Mtb* and in the vaccine strain *Mycobacterium bovis* BCG. *mtrA* transcription is sharply up-regulated in *M. bovis* BCG upon its entry into MΦ. In contrast, *mtr*A transcription is unchanged in virulent *Mtb* upon its infection of murine or human monocyte-derived MΦ (6, 7). These initial insights suggested to us that it is the activity of the MtrAB system, along with a few other key regulators, that is necessary for dictating the outcome of proliferation and persistence upon infection.

Because *mtr*A is an essential gene and the conditional knock-out strains of *mtr*A are unavailable, to address the roles of the *mtr*A gene product in *Mtb* proliferation upon infection, we created and characterized the *mtr*A merodiploid strains producing elevated levels of MtrA (8). These studies revealed that the merodiploid strain overproducing WT MtrA, designated as Rv78 *Mtb*(MtrA$^+$), is attenuated in MΦ and in mouse lungs, but it is otherwise as proficient as the WT strain for growth in nutrient broth. In contrast, the merodiploid overproducing phosphorylation-defective MtrA, due to a mutation at the phosphate accepting amino acid Asp-53 (8) and designated as Rv129 *Mtb*(D53N MtrA$^+$), is not severely attenuated in MΦ (8). We also found that the merodiploid overproducing both the WT MtrA RR and the MtrB kinase is as proficient as the WT

* This work was supported, in whole or in part, by National Institutes of Health Grants AI 084734 and AI 73966 (to M. V. M.) and AI 48417 (to M. R.). This work was also supported by Canadian Institutes for Health Research Operating Grant MT-13453 (to M.-C. O., D. P. B., and G. T. M.).

[S] The on-line version of this article (available at http://www.jbc.org) contains supplemental "Methods" and Figs. S1–S8.

[1] To whom correspondence should be addressed. Tel.: 903-877-2877; Fax: 903-877-5369; E-mail: murty.madiraju@uthct.edu.

[2] The abbreviations used are: MΦ, macrophages; 2CRS, two-component regulatory systems; RR, response regulator; ChIP, chromatin immunoprecipitation; WT, wild type; kan, kanamycin.

TABLE 1
Oligonucleotide primers used for ChIP assays

Primers	Gene/DNA	Remarks
1. Q21: gaggatcgcgagccgttgcc	*dna*A promoter-	Forward primer, 180-bp
2. MVM97: cggggtcatcggtcaacgacg	*dna*A promoter	Reverser primer
3. Mty51: ggggaattcttaaaaaaacttctc	*ori*C	Forward, 182-bp
4. MTBOriTF189RC: gtcggagttgtggatg	*ori*C	Reverse
5. P85b.F: ccaagctcgaatctttcggctcacgtctgtc	*fbp*B promoter	Forward, 202-bp
6. P85bR: ccgcgatagatccataccgccataccgtttg	*fbp*B promoter	Reverse
7. P85A.F: gtgacggcgccacgaaccctgtcaa	*fbp*A promoter	Forward, 209-bp
8. P85A.R: ttggccgtgaacgaccgccggataagggtt	*fbp*A promoter	Reverse primer
9. mtp210F: ctgtgtcgcggctacgacgtg	*mtr*A promoter	Forward, 223-bp
10 mtp415R: gggtcacgctgggcacggcc	*mtr*A promoter	Reverse
11. *mce*1AF: tgcacgatccgcaacttct	*mce*1 promoter	Forward, 220-bp
12. *mce*1AR: tcctcagcgagtagccgttac	*mce*1 promoter	Reverse, 220-bp
13. MVM238 gcggatccgcttcctccctggtggggc	*fts*Z promoter	Reverse, 160-bp
14. MVM508FZPE: tgcccgccgcgtatcggcgc	*fts*Z promoter	Forward,
15. pfbpCF: ttgcgccgctcgggagccagcc	*fbp*C promoter,	forward, 200-bp
16. p85CR: actctcatctgccgcacgacgcggtcgaat	*fbp*C promoter,	reverse
17. YneApSpeI: tggcaacactagtccggctgtccgcaccagcggc	*chi*Z promoter	forward, 198-bp
18. YneA2HIIIR: gtctcaagcttctcagacggtaatcgctcgcgtg	*chi*Z promoter	Reverse
Oligonucleotide primers used for qRT-PCR		
1. FbpA	Forward primer: 85AF:	5′-GGATCTGGGTGGCAACAACCT-3′
	Reverse primer: 85AR:	5′-CAGCTGTGCGTACCGCTGTC-3′
	RT primer: 85ART:	5′-GTTGCAGGTCGGGCTTCATAG-3′
	Taqman Probe: 85A.TP:	5′-TGCTGGTCCGCACGAAGCCCTCGA
2. FbpB:	Forward primer: MVM54685RTY1	5′-TCAGGGGATGGGGCCTAGCC-3′
	Reverse pimer:RTAg85A2	5′-GCTTGGGGATCTGCTGCGTA-3′
	RT primer:MVM545A85BRTY3	5′-GCCGGCGCCTAACGAACTCTGC-3′
	Taqman Probe: 85B-TP	5′-FAM-TCGAGTGACCCGGCATGGGAGCGT-BHQ-1 3′
3. 16S rRNA:	Forward primer: RT16S1:	5′-GAGTGGCGAACGGGTGAGTAACA-3′
	Reverse primer: RT16S2	5′-CACCCCACCAACAAGCTGATAGG-3′
	RT primer: RT16S3	5′-CCGCACGCTCACAG-3′
	Taqman Probe:	5′-FAM-d(TCCACCACAAGACATGCATCCCGTG)-BHQ-3′

strain for growth in MΦ (8). These studies lead to a hypothesis that optimal proliferation of *Mtb* in MΦ and in murine lungs depends, in part, on the ratio of phosphorylated MtrA (MtrA∼P) and nonphosphorylated MtrA and that MtrB kinase regulates the MtrA∼P state (8).

It is reasonable to assume that the essential RR MtrA or its MtrA∼P form regulates the activities of several essential targets and their associated pathways. A consequence of this regulation could determine whether the bacterium maintains a persistent state or assumes active multiplication and causes disease. A first step in understanding how MtrA RR might control *Mtb* proliferation upon infection is to identify the targets and define the DNA-binding motifs recognized by the MtrA RR. This study addresses these issues, and we demonstrate that *oriC*, the site where chromosomal DNA replication initiates, and *Pfbp*B, the promoter for a major secreted antigen 85B, are physiologically significant MtrA targets. Our work also identifies the MtrA DNA recognition motifs, and it is thereby an important step toward understanding the whole MtrA regulon and potentially how *Mtb* physiology is regulated between acute and latent disease states.

MATERIALS AND METHODS

Bacterial Strains—M. tuberculosis strain H37Rv was grown in Middlebrook 7H9 media. *Mtb mtr*A merodiploid strains were created by plasmid transformation, and transformants were selected on Middlebrook 7H10 agar supplemented with hygromycin (50 μg/ml) as described previously (8). *Escherichia coli* Top-10 were used to propagate mycobacterial plasmids.

Chromatin Immunoprecipitation Experiments—Our basic protocol as applied to *Mtb* cells was described previously (8). *Mtb*(MtrA$^+$) cultures (*Mtb* merodiploid overproducing WT MtrA protein) actively growing in Middlebrook 7H9 broth were exposed to 1% formaldehyde for 20 min and processed to prepare cellular lysates, and the genomic DNA was then sheared to an average size of 500 to 1000 bp, as described. Cleared supernatant was obtained and incubated with anti-MtrA or mock antibodies followed by immunopure protein G-agarose beads to collect immunoprecipitates. DNA samples were then purified using DNAzol, and protein-DNA cross-links were reversed by heating, and an aliquot of DNA was directly used to amplify select DNA fragments by PCR. The oligonucleotide primers that were used are listed in Table 1. PCR products were resolved in agarose gels, stained with SYBR Green, and photographed as needed. Typically, 30 cycles of amplification with serially diluted DNA of mock, immunoprecipitation-treated and total input samples were carried out. DNA band intensities were quantified by densitometry scanning and analyzed by Molecular Imager Fx. Typically, DNA samples were diluted 100- and 200-fold and used in PCR. The band intensities for FtsZ are the same with anti-MtrA and mock antibodies, *i.e.* not enriched with anti-MtrA antibody (8). We considered this ratio as 1 and normalized the same ratio for each of the other targets to this value. For all initial experiments, values 2 and above were considered as potential MtrA targets.

RNA Extraction and Quantitative Real Time-PCR Analysis—Extraction of total *Mtb* RNA from Middlebrook 7H9 broth-grown and intracellular macrophage-grown cells was done essentially as described previously (8). DNA contamination was removed by treatment with DNase I (Ambion). Approximately 50–100 ng of total RNA was reverse-transcribed to make cDNA specific to *fbp*B, *fbp*A, and 16 S rRNA genes using Superscript II reverse transcriptase (Invitrogen). Target cDNA from

control and experimental sets were amplified in separate reaction tubes. Real time PCR (TaqMan® chemistry) was carried out in a Bio-Rad I-Cycler using the *Taq*DNA polymerase (New England Biolabs), TaqMan® probes (Biosearch Technologies), and reverse and forward primers (see Table 1). The calculated threshold cycle (*Ct*) value for each gene of interest was normalized to the *Ct* value for 16 S. and the fold expression was calculated using the following formula: fold change $= 2^{-\Delta\cdot(\Delta Ct)}$. No reverse transcription reactions were included as negative controls. Expression data are the average from three independent RNA preparations, each reverse-transcribed and quantified by real time PCR in triplicate.

oriC Plasmid Mutagenesis and Autonomous Replication Analysis—pMQ219 is the *Mtb ori*C plasmid that has an 814-bp DNA fragment containing the 150-bp 3′-end of the *dna*A, the 115-bp 5′-end of the *dna*N, and the 553-bp their intergenic region (9). Mutations in the MtrA-boxes F2, F3, F4, and F5 were created by PCR mutagenesis following the previously described protocols (8, 10–12). The "GTCACA" nucleotides of the selected MtrA-boxes in all cases were replaced with a "TATATA" sequence. Plasmid pMMR87 carries mutations in MtrA-box F2, whereas pMMR88 contains mutations in F2, F3, F4, and F5. The integrity of the cloned insert and the mutated residues was confirmed by DNA sequencing. Approximately 250 and 500 ng of *ori*C plasmid DNA was used to electrotransform *Mtb* H37Rv (WT), Rv19 (*Mtb* carrying integrated plasmid lacking the *mtr*A insert), Rv78 (*Mtb* MtrA$^+$), and Rv129 (*Mtb* MtrAD53N) strains, and transformants were selected on Middlebrook 7H10 agar plates containing 10 μg/ml kanamycin (kan) for WT or 10 μg/ml kan and 50 μg/ml hygromycin for Rv19, Rv78, and Rv129. Both Rv78 and Rv129 strains showed poor transformation efficiency. The pZErO 2.1 plasmid was always used as a control. Measurement of transformation frequency, recovery of *ori*C plasmids, and Southern analysis were performed essentially as described previously (9, 13).

oriC Plasmid Stability Experiments—Actively growing cultures of *Mtb* merodiploid strains producing normal levels of MtrA (Rv19), elevated levels of phosphorylation-competent *Mtb*(MtrA$^+$), and phosphorylation-defective *Mtb*(D53N, MtrA$^+$) MtrA proteins in Middlebrook 7H9 broth containing kan were seeded into fresh growth media lacking kan and grown for different days. At indicated time intervals, aliquots of cultures were removed, diluted, spread on agar plates containing hygromycin, but with and without kan, and incubated at 37 °C for 3 weeks. Colonies from both series of plates were counted, and the proportion of kan-resistant colonies was determined.

DNase I Footprinting Analysis—DNase I protection footprint assays were done as described previously (14). The ^{32}P-5′-end-labeled DNA fragments containing the *Mtb ori*C and the *fbp*B promoter were prepared as described previously (14). The *ori*C end-labeled DNA fragments were prepared from plasmid pMQ219 (9), which contained the same 814 bp of *Mtb ori*C DNA used for the autonomous replication experiments. The ^{32}P-5′-end label was placed at the polylinker EcoRI (*dnaA* 3′) site or at the HindIII (*dnaN* 5′) site (Fig. 3) and at the natural *ori*C SalI or HpaII sites (footprints not shown). The *fbp*B promoter end-labeled DNA fragments were prepared from plasmid pGEMT-*fbp*B and were created by ligating PCR-amplified DNA (a 202-bp fragment amplified by P85bF and P85bR, see primers in Table 1) into the TA overhang plasmid pGEMT-easy (Promega). The ^{32}P-5′-end label was placed at the polylinker NcoI site (Fig. 2) or at the polylinker NdeI site (footprints not shown). Both plasmids pMQ219 and pGEMT-*fbp*B were sequenced prior to footprint analysis.

In Vitro MtrA Protein Purification and Phosphorylation—The pET plasmid overexpressing His-tagged MtrA protein from a T7 promoter was described previously (8). This plasmid was transformed into the ArcticExpress (DE3) RIL strain (Stratagene, catalog no. 230193), and MtrA overproduction was induced by adding 1 mM isopropyl 1-thio-β-D-galactopyranoside to actively growing cultures at 30 °C and grown for 20 h at 10 °C. The recombinant His-MtrA protein was purified on nickel affinity columns as described previously (8). MalE-EnvZ kinase purification and MtrA phosphorylation by EnvZ protein were essentially performed as described previously (8).

RESULTS

MtrA Phosphorylation Levels and Intramacrophage Growth—Our approach for identifying MtrA RR targets is first to define growth conditions where MtrA phosphorylation-dependent phenotypes are evident and then to infer potential targets and to test them by biochemical and *in vivo* approaches. Earlier experiments to evaluate the consequences of MtrA overproduction used THP-1 cell lines, which may not have all of the properties of immunoactive MΦ (8). To confirm these findings in a more native system, we evaluated the growth kinetics of *Mtb* merodiploids producing elevated levels of WT phosphorylation-competent WT MtrA (Rv78) and *Mtb* merodiploids producing elevated levels of phosphorylation-defective D53N MtrA (Rv129) in human peripheral blood monocyte-derived macrophages. Similar to the results reported with the THP-1 cell lines, the Rv129 merodiploids replicated proficiently in monocyte-derived cells, whereas the Rv78 merodiploids did not (supplemental Fig. S1). These results further support our working hypothesis that, during intracellular growth, the elevated pools of MtrA increase the levels of MtrA∼P and this in turn mis-regulates the targets of MtrA. Such targets could include genes for promoting intramacrophage growth and genes involved in the replication and cell division of *Mtb.*

ChIP Indicates That Chromosomal Replication Origin, oriC, and the Promoter for Antigen 85B Are MtrA Targets—Based on the above hypothesis, we focused the initial studies on two types of potential targets and analyzed them by ChIP. The first targets included the secreted antigen 85 complex pathway responsible for cell wall biogenesis, and the second targets included the DnaA-mediated *ori*C replication pathway. The antigen 85 family includes a family of proteins that bind fibronectin and are designated as *fbp*A, *fbp*B, and *fbp*C (15–17). These proteins catalyze mycolyl transferase activity (18), which is critical for generating α-α-trehalose dimycolate or "cord factor", a major virulence factor (19, 20). Also, infection of monocyte-derived macrophages with *Mtb* is shown to be associated with a sharp increase in the expression of *fbp*B, and such a rapid increase is believed to be necessary for establishing infection and subsequent proliferation in macrophages (21). The expression of

*fbp*A is differentially modulated during the acute and chronic stages of infection (22–24). Another critical point for regulating cell proliferation is *ori*C because it is the site where chromosomal DNA replication begins upon the binding of the initiator protein DnaA as well as several other global regulators that must coordinate replication with cell division (25–27). As additional potential MtrA targets, we selected the promoters of *dna*A, the initiator of DNA replication; *fts*Z, the initiator of cell division; Rv2719, a cell wall hydrolase regulating Z-ring assembly; *mce*1, the gene product required for *Mtb* invasion and possibly virulence (8, 28–30); and finally, *mtr*A, whose expression, like other RR genes, is expected to be autoregulatory (6, 7).

Fig. 1*A* shows representative ChIP data obtained with anti-MtrA antibodies. As shown, the PCR product signals of *ori*C and those of the *Pdna*A and *Pfbp*B were conspicuously increased by binding with anti-MtrA antibodies relative to the no antibody (mock) controls (Fig. 1*A*). The PCR signals for *P*Rv2719c, *PftsZ*, and *Pmce*1 remained unchanged, whereas those of the *Pfbp*A and *Pfbp*C increased modestly relative to the controls (Fig. 1*A*). Finally, the signal for the *Pmtr*A region was also enriched (Fig. 1*A*), consistent with the hypothesis that expression of *mtr*A, like other RR, is autoregulated. To obtain consistent and statistically significant results, we measured the anti-MtrA to mock ratio by densitometric scanning and normalized the data to that of a negative control, the *PftsZ* ratio. From four independent experiments, we obtained the ratios for *ori*C (2.6), *Pfbp*B (2.5), *Pdna*A (2.0), and *Pmtr*A (2.9), whereas those of the *Pfbp*A (1.6) and *Pfbp*C (1.6) were below 2.0 (see Fig. 1*B*). For initial characterization, we focused on *Pfbp*B and *ori*C, whose ratios were significantly higher than 2.0.

We supported our ChIP results with electrophoretic mobility shift assays, and we evaluated MtrA binding to *ori*C with both MtrA and MtrA∼P (phosphorylated MtrA). The MtrA∼P was produced by incubating MtrA with heterologous kinase EnvZ and ATP (8). Incubation of these proteins with the fluorescein isothiocyanate-labeled *ori*C DNA fragment led to a protein concentration-dependent retardation in the mobility (supplemental Fig. S2). Less MtrA∼P than MtrA was required to shift the *ori*C DNA, demonstrating that phosphorylated MtrA acquires a higher affinity for *ori*C-binding sites. Similar results were obtained with the *fbp*B promoter (data not shown). Together, these *in vitro* electrophoretic mobility shift assays and *in vivo* ChIP data demonstrate that both *ori*C and the *Pfbp*B are significant MtrA targets.

DNase I Footprinting Reveals MtrA-binding Sites—Next, we performed DNase I protein footprinting experiments to identify the MtrA-binding sites in *fbp*B and *ori*C. MtrA or MtrA∼P was added to binding reactions with ^{32}P-5′-end-labeled DNA targets. Figs. 2 and 3 provide examples of DNase I protection footprinting experiments in the *Pfbp*B 5′ and the *ori*C regions. As can be seen, MtrA produces one long footprint (a span of DNase I protection) from 91 to 149 bp upstream of *fbp*B. This binding requires ATP (Fig. 2*A*), implying that phosphorylated MtrA∼P gains significant affinity for *fbp*B target DNA. We did not observe this footprint when ATP was omitted. Assuming 100% MtrA phosphorylation, then MtrA∼P binds *fbp*B with an apparent K_d ∼10 nM. However, this K_d is a large overestimate.

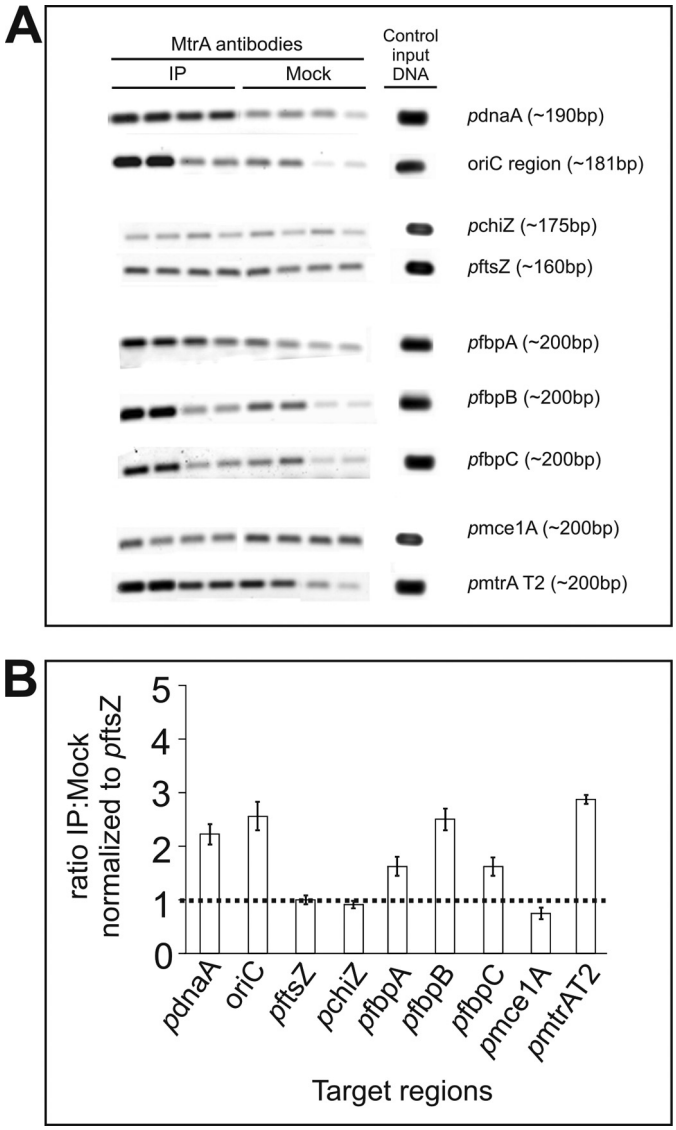

FIGURE 1. **ChIP experiments.** *A,* agarose gel analysis of ChIP samples. *Mtb* cell lysates following formaldehyde cross-linking, immunoprecipitation (*IP*) with anti-MtrA or mock antibodies, and heat reversal of cross-links were used in PCR with select targets. Lysates were diluted 50- and 200-fold for *ori*C and the promoters of *fts*Z, *dna*A, chiZ, *fbp*A, *fbp*B, and *fbp*C promoters. For *mtr*A promoters, 100- and 300-fold diluted lysates were used. PCRs were done in duplicate, and products were resolved by agarose gel electrophoresis, stained with SYBR Green dye, and visualized by scanning in Molecular Imager Fx. Product lanes corresponding to anti-MtrA and Mock antibodies and the target in question are marked. *Control input DNA* refers to PCR products wherein an aliquot of suitably diluted genomic DNA was used with appropriate primers in amplification reactions. Representative data for each target are shown. *B,* normalization of ChIP data. PCR products obtained were scanned by densitometry and analyzed by Quantity One software (Bio-Rad Molecular Imager Fx). The ratio of anti-MtrA to mock immunoprecipitation signals was determined for each primer pair and normalized against that of the FtsZ promoter value. The *y* axis shows the normalized anti-MtrA to mock ratio, and the *x* axis shows the individual targets.

Our unpublished phosphate transfer experiments[3] estimated that only ∼1% of MtrA was phosphorylated in these and similar binding assays. Therefore, MtrA∼P affinity is very high, with apparent K_d values around 0.1 nM.

[3] M. Rajagopalan and M. V. Madiraju, unpublished data.

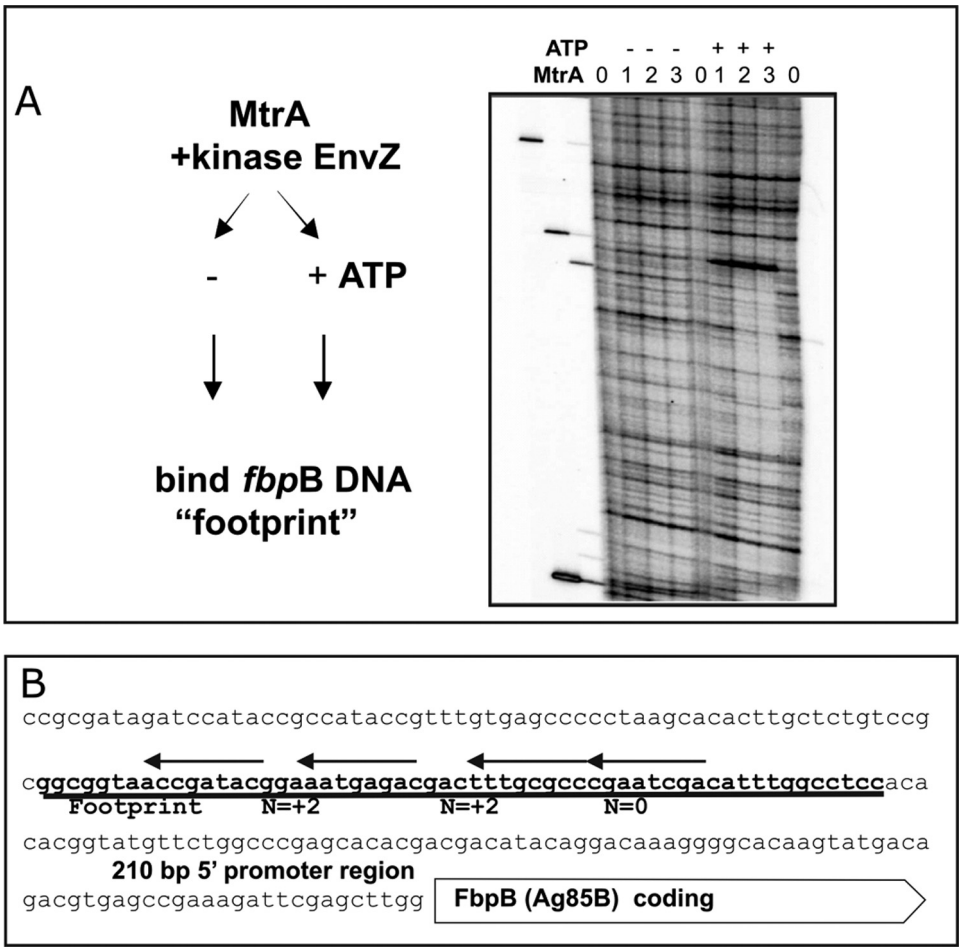

FIGURE 2. **MtrA footprint analysis in the 5′ region of *fbp*B (Ag85B).** *A,* MtrA binding requires ATP in the protein kinase reaction. Purified His-tagged MtrA protein was phosphorylated by incubation with soluble maltose-binding protein-tagged *E. coli* EnvZ kinase and 1.0 mM ATP for 30 min prior to the DNase I protection "footprint" analysis using the ^{32}P- 5′-end-labeled DNA fragment, as detailed under "Materials and Methods," which spans the upstream region of *fbp*B. The numbers (*0, 1, 2, 3*) *above* the lanes indicate that either 0, 10, 20, or 30 μl of the phosphorylated MtrA (2 mg/ml MtrA protein) was added to the standard 200-μl binding reactions. The − or + signs indicate that ATP was either absent or present in otherwise identical reactions. *B,* DNA sequences bound by MtrA. The DNA sequences immediately upstream to the annotated *M. tuberculosis* FbpB coding DNA are shown. The zone of MtrA-specific DNase I protection, presented above in footprints A and B, is *underlined*. The *arrows* above this footprint align with the best matches to the direct repeats (with variable $n = 2$ or $n = 0$ bp spacing). These are the proposed MtrA recognition sequences that are described in the text and in Fig. 5.

The MtrA protected region is marked with bold line in the ag85B sequence (Fig. 2*B*). Our MtrA DNA-binding sequence analysis (see below) predicts four direct repeat binding motifs under this long footprint.

Similar footprint experiments in the *ori*C region produced multiple MtrA footprints (Fig. 3). These experiments used ^{32}P-5′-end-labeled DNA on either side of *ori*C (number 1, inside the 5′ start of *dnaN,* and number 2 inside the 3′-end of *dnaA*). In similar footprint experiments, we also used ^{32}P-end-labeled DNA inside *ori*C at the HpaII and SalI sites (Fig. 3*B*) (data not shown). The positions of these footprints are summarized in Fig. 3*C*. Although the single *fbp*B 5′ footprint was 60 bp long (Fig. 3*C*), the *ori*C footprints were less than half this length, and we distinguished two lengths. Spans of 20–30 bp were labeled as "Footprints" (F1, F2, F3, F4, F5, F6A, and F6B), which are marked as *solid lines* in Fig. 3*C*. Spans of less than 10 bp were labeled as "Toe prints" (T1, T2, T3, T4, and T5), and these are marked as *dotted lines* in Fig. 3*C*.

MtrA-binding Sequences—Next, we performed multiple sequence alignments of the MtrA footprinted DNA to identify the common DNA sequences recognized by MtrA. This analysis suggested that MtrA-binding sites were organized as 9-bp direct repeats (Fig. 4), and six of the *ori*C footprints span two 9-bp direct repeats with either an $n = +2$, $n = 0$, or an $n = -2$ spacing. A base pair frequency analysis of these aligned direct repeats suggested a consensus GTCACAgcg, and a Logo analysis also argued that most of the recognition information lies in the first six positions GTCACA (Fig. 4). The MtrA-binding sites under the *fbp*B (Ag85B) footprint can also be viewed as four of the same direct repeats with $n = 0, +2, +2$ spacing, but these direct repeats show more differences from the consensus (compare Fig. 2*B* with Fig. 4). If one MtrA molecule binds one DNA direct repeat, then four MtrA molecules bind the *fbp*B (Ag85B). This assumption agrees with the extra length of this footprint. Also, the strict requirement of ATP (MtrA∼P) for binding *fbp*B (Fig. 2*A*) suggests an extra cooperative mode of binding by MtrA molecules at *fbp*B. This view is further supported by the electrophoretic mobility shift assay results in supplemental Fig. S3, where MtrA forms two shifted DNA complexes with *fbp*B DNA but only one shifted-DNA complex with an *ori*C-binding site, for example.

Next, we evaluated the importance of the spacing between the direct repeats (supplemental Fig. S4). For example, the *ori*C footprint F2 with $n = 0$ spacing has the closest matching direct repeats (two perfect GTCACAnnn motifs), but F2 occupancy is barely detectable in Fig. 3*A* (*#2*). At the same MtrA∼P concentrations, F1 with $n = +2$ bp spacing is almost fully occupied. Accordingly, we asked if MtrA affinity for F2 would increase with an alternative $n = +2$ spacing by using electrophoretic mobility shift assays (supplemental Fig. S4). Double-stranded DNA oligonucleotides were modeled after the *ori*C F2 DNA. Two GTCACAnnn direct repeats with $n = 0$ (WT) spacing and with $n = +2$ bp spacing were incubated with serial 1:3 dilutions of an MtrA kinase reaction. Although selective MtrA binding to the WT *ori*C F2 ($n = 0$) DNA was barely detectable (supplemental Fig. S4), MtrA affinity for *ori*C F2 + 2 DNA was substantial, and only these binding reactions could produce reliable K_d measurements (supplemental Fig. S3). MtrA affinity requires both optimal spacing and correct sequence motifs

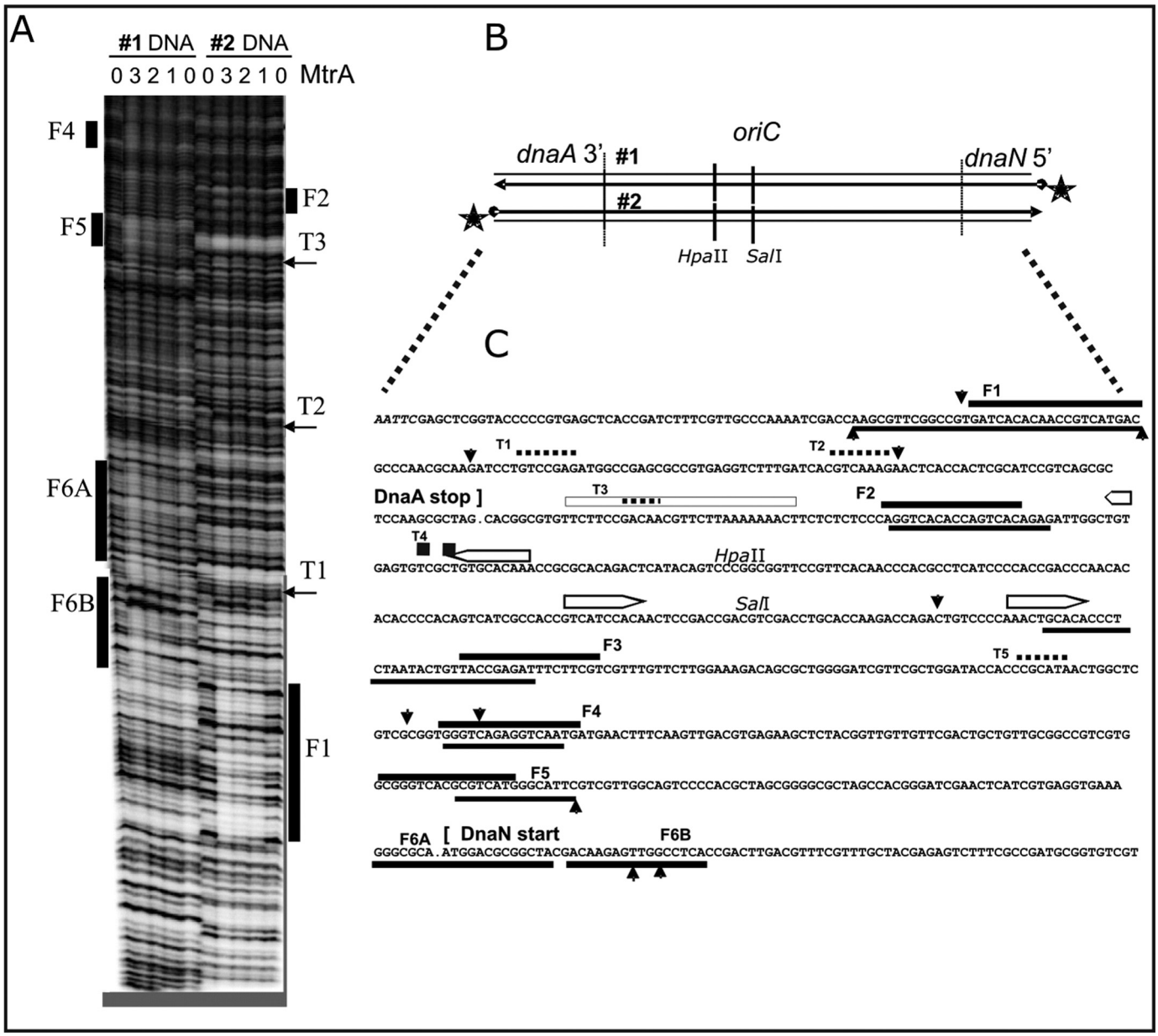

FIGURE 3. **MtrA footprint analysis in the *M. tuberculosis ori*C region, between 3′ *dnaA* and 5′ *dnaN*.** *A*, two representative autoradiograms (*#1* and *#2*) using ^{32}P-5′-end-labeled DNA, diagrammed in *B*, at the 5′-end of *dnaN* (*#1*) and the 3′-end of *dnaA* (*#2*). Purified His-tagged MtrA protein was phosphorylated as described in Fig. 2, prior to the DNase I protection footprint analysis, also detailed under "Materials and Methods." The numbers (*0, 1, 2, 3*) *above* the lanes indicate that either 0, 10, 20, or 30 μl of the MtrA (2 mg/ml protein) was added to the standard 200-μl binding reactions. Similarly aligned *bars* and arrows mark the footprints (F1, F2, … F6A, F6B) and shorter toe prints (T1, T2 …) that are described in the text and aligned with the DNA sequence in *C*. *B*, schematic diagram of the *M. tuberculosis ori*C region is aligned with the ^{32}P-end-labeled DNA (*#1* and *#2*) used in *A*. The indicated HpaII and SalI sites also served as positions for ^{32}P-end-labeled DNA used in additional footprint experiments not shown. *C*, summary of MtrA footprint analysis in the *M. tuberculosis ori*C region. These DNA sequences correspond with the above *ori*C schematic in *B* and with the footprints in *A*. It also summarizes footprint experiments (using internally labeled HpaII and SalI sites) that are not shown. The *open bars with pointed ends* mark established DnaA-boxes (9). *Solid bars* mark the footprints (F1, F2, … F6A, F6B), and *dotted lines* mark the shorter toe prints (T1, T2 …). *Perpendicular arrowheads* mark the prominent DNase I cut sites that are enhanced by MtrA. When positioned below the presented DNA sequences, these *lines* and *arrows* indicate the sequences protected or cleaved on the corresponding bottom strand.

because selective binding is lost with mutant F2 + 2 DNA that has one altered direct repeat motif (supplemental Fig. S4).

Transcription of fbpB Is Sharply Decreased during Intramacrophage Growth in mtrA Merodiploid Overproducing WT MtrA—As reviewed, the transcription of *mtr*A in virulent *Mtb* remains unchanged in broth and during intra-MΦ growth, whereas the *fbp*B expression is up-regulated upon infection (6, 7, 31). DNase I footprinting data (Fig. 2) imply that *fbp*B transcription is regulated by MtrA. To test this possibility, we examined the quantitative real time-PCR expression profile of *fbp*B from intramacrophage and broth-grown bacteria relative to the housekeeping gene, 16 S rRNA. The fold-differences in the *fbp*B expression in MΦ relative to broth condition are presented (Fig. 5*A*). The *fbp*B expression relative to 16 S rRNA was up-regulated upon infection in WT cells producing normal levels of MtrA and MtrB, confirming the published data of Wilkinson *et al.* (21). In contrast, the *fbp*B expression was down-regulated in Rv78 *Mtb*(MtrA$^+$) merodiploids overpro-

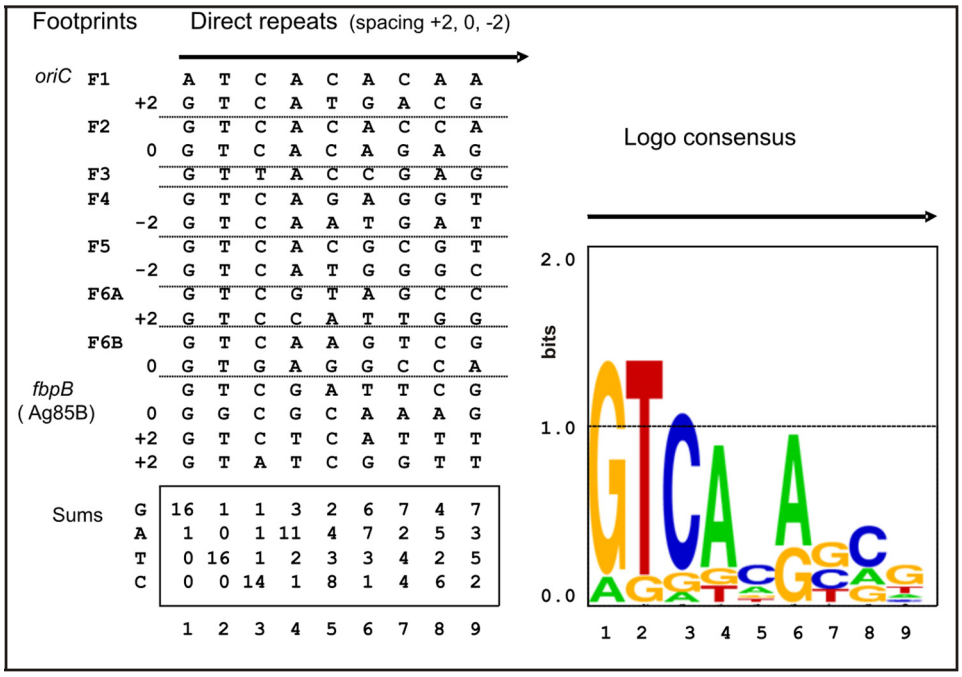

FIGURE 4. **Motif log analysis.** MtrA binds by apparently recognizing two or more direct repeats similar to GTCACA. The DNA sequences under the footprints in Figs. 2 and 3 were aligned to assume optimum similarity. For 6 out of the 7 *ori*C footprints, shown in Fig. 3*C*, the best aligned DNA could be organized as two direct repeats, but a variable spacing of +2, 0 or −2 bp was required for alignment. The exceptional footprint F3 apparently contained only one direct repeat. Frequency and Logo analysis suggests that most of the sequence conservation and presumably most of the information that specifies selective DNA binding lies in the first six positions (GTCACA). Four similar but less exact direct repeats with $n = 0$, $n = +2$, and $n = +2$-bp spacing are also present under the MtrA footprint 5′ to *fbp*B (Fig. 3*C*). The supplemental Fig. S3 demonstrates that the $n = +2$-bp spacing provides a higher affinity than $n = 0$.

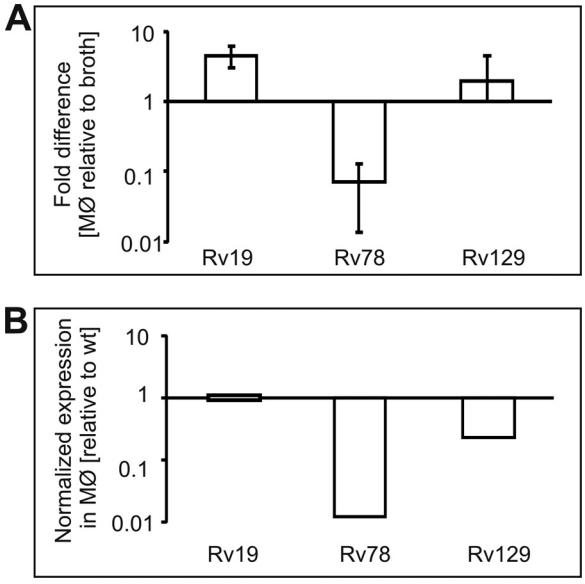

FIGURE 5. **Quantitative real time-PCR analysis of *fbp*B gene expression.** The cDNA specific to *fbp*B and 16 S rRNA genes was synthesized from the RNA samples of Rv19 *Mtb* (WT), Rv78 *Mtb*(MtrA$^+$), and Rv129 *Mtb* (D53N MtrA$^+$) strains grown in broth and macrophages and used to evaluate *fbp*B expression relative to 16 S rRNA. Data are presented as fold-differences in the expression of macrophage-grown bacteria relative to broth (*A*). The *fbp*B RNA expression data of Rv78 and Rv129 were normalized against the wild type strain and are also presented (*B*).

ducing MtrA (in cells producing normal levels of MtrB) upon infection, although it was restored to near WT levels in the Rv129 *Mtb*(D53N MtrA$^+$) merodiploids (Fig. 5*A*). When normalized to WT, the *fbp*B expression in Rv78 was found to be reduced nearly 70-fold (see Fig. 5*B*). These results suggest that a consequence of MtrA overproduction leading to an imbalance between MtrA and MtrA∼P levels is reduction of *fbp*B expression.

Mutations in MtrA-boxes Compromise oriC Plasmid Replication—To test how MtrA-boxes (or direct repeats, Fig. 4) might influence autonomous replication, *ori*C plasmid replication assays were performed with both WT and altered *ori*C DNA. Previous studies showed that *E. coli* plasmids do not replicate in *Mtb* and other mycobacterial species (9, 13, 32). However, such plasmids with an 814-bp DNA *Mtb ori*C fragment containing the 3′-end of *dna*A, the 5′-end of *dna*N, and their intergenic region (pMQ219), maintain stable autonomous replication (9, 13). Previous studies also showed that mutations in individual DnaA-boxes, but not in areas located outside the DnaA-boxes, decrease transformation efficiency and autonomous replication activity, indicating that DnaA-boxes are critical for *ori*C plasmid replication (9, 13, 33). To test if MtrA-boxes are similarly important, we created two plasmids, one containing mutations in the MtrA-box F2 (pMMR87, see Fig. 6, *A* and *B*) and the other containing mutations in MtrA-boxes F2, F3, F4, and F5 (pMMR88, see Fig. 6, *A* and *B*). The F2-box, although it showed weak affinity to MtrA, is highly conserved in all mycobacterial species, including *Mycobacterium leprae* (see supplemental Fig. S5). The GTCACA sequence of the MtrA motifs was replaced with TATATA in both plasmids (see Fig. 6*B*).

Consistent with the published reports, transformation of WT *Mtb* with the pMQ219 plasmid gave several kan-resistant transformants with a transformation frequency of 10^4 colonies/μg input DNA (9, 33). The pMQ219 input plasmid was recovered in *E. coli* when the total DNA preparation of the pMQ219 transformants was used to transform the *E. coli* Top-10 strain, indicating that this plasmid replicates autonomously in *Mtb*. In contrast, transformation of *Mtb* with the pMMR87 and pMMR88 plasmids produced tiny pin-headed colonies, indicating a growth defect from an inability to maintain these *ori*C plasmids. Transformation of *E. coli* with the total DNA extracted from the primary transformants collected from several plates failed to produce kan-resistant colonies, indicating that the mutant MtrA plasmids could not be recovered and were therefore not replicating autonomously in *Mtb* (data not shown). PCR analysis with oligonucleotide primers specific to the *ori*C or to the kan cassette yielded positive signals

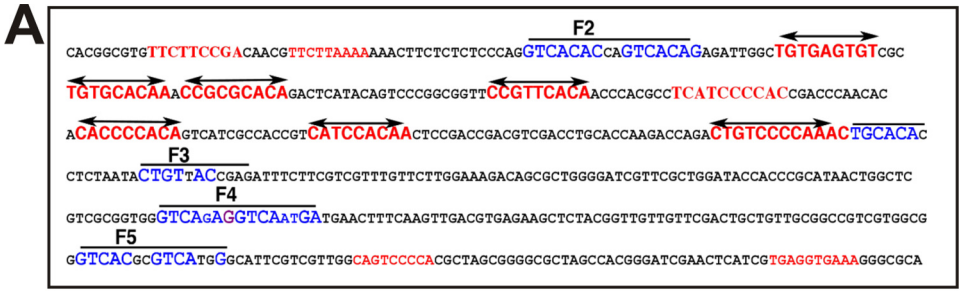

B

MtrA motif sequence	Mutated sequence in plasmid	
F2: GTCACACCAGTCACAG	TATATACCATATATAT	pMMR87
F2: GTCACACCAGTCACAG	TATATACCATATATAT	pMMR88
F3: TGCACACCCTCTGTTAC	TATATACCCTATATAC	pMMR88
F4: GTCAGAGGTCAATGA	TATATAGTATATATA	pMMR88
F5: GTCACGCGTCATGGG	TATATACTATATAT	pMMR88

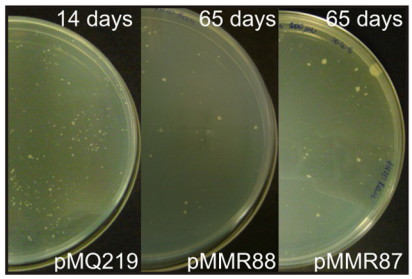

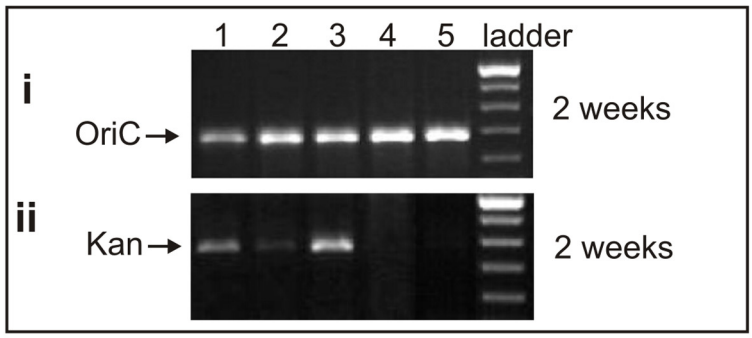

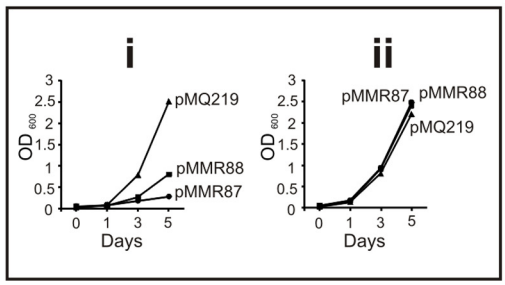

FIGURE 6. ***oriC* sequence, MtrA direct repeat mutations, and *oriC* plasmid transformation assays.** *A, oriC* sequence (the *dnaA-dnaN* intergenic region). DnaA-boxes are marked in *red,* and MtrA-boxes are marked in *blue*. Mutated residues in the MtrA-boxes F2, F3, F4, and F5 are shown. *B,* mutated MtrA-box sequences. The presumptive MtrA motifs and the sequences of the mutated boxes are shown for clarity. The plasmid pMMR87 contains only the first F2 mutation and pMMR88 contains all four mutations. *C, oriC* transformants on agar plates. Approximately 250 ng of WT (pMQ219) and mutant (pMMR87 and pMMR88) plasmid DNA was electrotransformed into *Mtb* H37Rv WT, and plates were incubated at 37 °C. The pMQ219 transformants in WT background were photographed after 14 days, and the pMMR87 and pMMR88 transformants were photographed after 65 days. *D,* agarose gel showing *oriC* and kan cassette PCR products. Genomic DNA of the transformants of pMQ219, pMMR87, pMMR88, and control pZErO 2.1 were extracted and used as templates to amplify *oriC* (*panel i*) and the kan cassette (*panel ii*). The PCR products were resolved on 0.8% agarose gels, stained with ethidium bromide, and photographed. *Lane 1,* pMQ219; *lane 2,* pMMR87; *lane 3,* pMMR88; *lane 4,* Rv WT; *lane 5,* pZErO 2.1; *lane 6,* 1-kb DNA ladder. *E,* growth curves of *Mtb* merodiploid strains. The frozen stocks of pooled transformants of pMMR87 and pMMR88 were diluted in Middlebrook 7H9 broth supplemented with oleic acid/dextrose/albumin/sodium chloride with 10 μg/ml kan (in *panel i*) and without antibiotic (in *panel ii*) and grown for 10 days to a final A_{600} between 0.25 and 0.3. The cultures were then diluted to A_{600} of 0.05, and the growth was monitored daily, as shown. For pMQ219, the freezer stocks were diluted and grown for 3 days to A_{600} of 0.6 prior to diluting to a final A_{600} of 0.025. Note that the growth rates of these cultures are very similar when grown in the absence of antibiotic. Similar results were also obtained when antibiotic concentration was increased to 25 μg/ml (data not shown).

(Fig. 6*D, panels i* and *ii*), like the WT *ori*C plasmid, pMQ219, indicating that the mutant *ori*C plasmids were also present but presumably integrated into the chromosome. Incubation of transformation plates up to 65 days led to a modest increase in the size of the mutant *ori*C plasmid colonies (Fig. 6*C*, representative plate is shown). Consistent with the slow colony growth, the liquid broth growth rates of the pMMR87 and pMMR88 transformants were similarly decreased as compared with WT *ori*C pMQ219, but only when grown in the presence of kan for plasmid selection. No differences in the growth rates were observed when these same cultures were grown without kan (Fig. 6*E*). A similar PCR analysis of pMMR87 and pMMR88 transformants failed to detect plasmid, *i.e.* kan cassette after 65 days of incubation indicating plasmid loss (data not shown). Presumably, the presence of the integrated plasmid in these transformants is deleterious in itself. The inability to recover *ori*C plasmids with mutations in the MtrA-boxes combined with the slow growth of transformants suggests that the mutant plasmids are severely compromised for replication. In particular, pMMR87 demonstrates that mutations in only the one MtrA-box at F2 are sufficient to compromise replication.

Next, we examined the consequences of MtrA overproduction on *ori*C plasmid replication and its maintenance by transforming pMQ219 and pMMR88 plasmids into Rv78 and Rv129, which are *Mtb* merodiploid strains overproducing WT *Mtb*-(MtrA$^+$) and phosphorylation-defective *Mtb*(D53N, MtrA$^+$) MtrA proteins (8). As a control, these plasmids were also transformed into Rv19, which is WT *Mtb* carrying an integrated plasmid vector lacking the *mtr*A insert. Transformation of pMQ219 into Rv78 and Rv129 produced a similar number of transformants (~10^4 per μg of DNA) as compared with that into WT (data not shown) indicating that transformation efficiency of pMQ219 plasmid was not affected by MtrA overproduction. PCR analysis of merodiploid transformant genomic DNA confirmed the presence of *ori*C and kan cassettes of pMQ219 plasmid (Fig. 7*A*). Efforts to recover pMQ219 plasmid from all three strains were, however, unsuccessful indicating that the pMQ219 plasmid is not replicating extrachromosomally but rather is integrated on the chromosome. Southern analysis supported our interpretation that integration events may have occurred, because we identified the presence of bands corresponding to chromosomal *ori*C (~3 kb) and the integrated plasmid (~5.5 kb) (see supplemental Fig. S6, *A* and *B*). DNA band corresponding to ~4.2 kb would be detected if the pMQ219 plasmid were to be replicating extrachromosomally, and this is what we see in the *Mtb* WT background (supplemental Fig. S6*C*, also legend for more details). Because replication potential of the pMQ219 plasmid in Rv WT and Rv19 backgrounds appears to be different, for the sake of clarity, pMQ219 in WT background is referred to as free plasmid and that in Rv19, Rv78, and Rv128 is referred to as integrated plasmid. It is not readily evident why pMQ219 plasmid is excluded in the Rv19 background, and further studies are required to address this issue (see "Discussion").

Assuming that replication is initiated at both origins, *i.e.* native and integrated *ori*C, then such activated origins could compete for replication components and pose origin incompatibility issue (36). This could in turn have consequences on cell

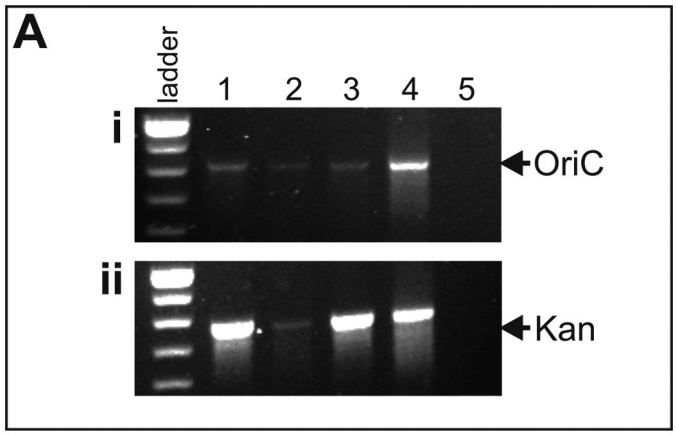

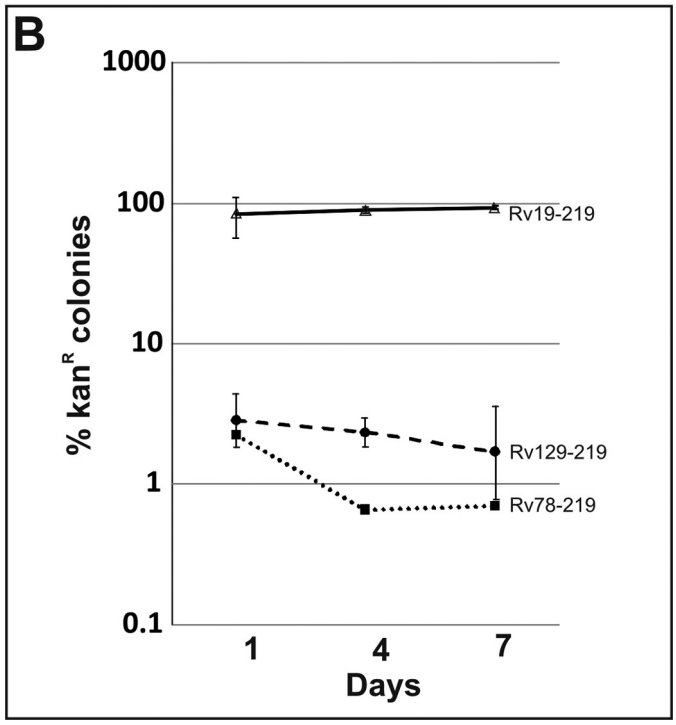

FIGURE 7. **Effect of MtrA overproduction on pMQ219 plasmid stability.** *A,* agarose gel showing *ori*C and kan cassettes. Genomic DNA preparations of *Mtb* merodiploid strains overproducing WT *Mtb*(MtrA$^+$) and phosphorylation-defective *Mtb*(D53N, MtrA$^+$) MtrA proteins, along with the control (RV19), were analyzed by PCR for *ori*C (*panel i*) and kan (*panel ii*). *Lane 1,* Rv19; *lane 2,* Rv78; *lane 3,* Rv129, *lane 4,* pMQ219 plasmid; and *lane 5,* Rv WT. *B,* stability experiments are as follows: *Mtb* merodiploids actively growing in broth in the absence of kan were diluted at indicated time periods, spread on agar plates with and without kan, and viable colonies appearing after 3 weeks incubation were determined. The ratio of kan-resistant colonies among total cells were presented on semi-log scale.

cycle progression and the stability of integrated plasmid sequences. To evaluate if integrated plasmids bearing *ori*C sequences are stably maintained, we carried out stability experiments. In these experiments, the pMQ219 merodiploid strains cultured in the absence of kan antibiotic for different days were spread on agar plates without and with kan. As can be seen, less than 5% Rv78 and Rv129 cells were kan-resistant, whereas nearly 100% Rv19 cells were kan-resistant (Fig. 7*B*). Although differences between the Rv78 and Rv129 strains were minor, plasmid loss in *Mtb*(MtrA$^+$) was relatively more than that in the *Mtb*(D53N, MtrA$^+$). These results indicate that the

pMQ219 plasmid remained relatively intact in cells producing normal levels of MtrA (Fig. 7*B*), but was lost significantly under MtrA overproduction conditions, and that MtrA phosphorylation has no effect on plasmid maintenance. Taken together, these results clearly reveal that optimal levels of MtrA are required for maintenance of plasmid bearing *ori*C sequences and that *ori*C is the MtrA target.

We also attempted to transform pMMR88 plasmid into Rv19, Rv78, and Rv129. Like the situation seen in the WT background, transformation of pMMR88 plasmid into Rv19 produced several tiny pinhead colonies that grew slowly, thus indicating a growth defect (data not shown). In the case of Rv78, we obtained in two independent experiments 12 and 90 transformants/μg of DNA, respectively, whereas with Rv129 we obtained after repeated attempts only 3 transformants/μg of DNA (data not shown). These results indicated that transformation efficiency of mutant *ori*C plasmids is severely compromised under MtrA overproduction conditions. The primary transformants grew slowly in liquid broth, but after repeated culturing began to grow like their WT counterparts. Presumably, the newly acquired growth advantage of these strains is due to accumulation of spontaneous mutations. Further studies are required to characterize these strains. Consequently, the pMMR88 transformants were not processed further.

DISCUSSION

In this study, we have identified and validated two important, but rather unrelated, sequences as MtrA targets. These are *ori*C, the DNA sequence critical for the initiation of chromosomal DNA replication and the duplication of genome, and the promoter for the *fbp*B gene, which codes for an immunodominant major secreted antigen 85B. Initial *in vivo* ChIP experiments (Fig. 1) were supported by *in vitro* DNase I footprinting (Figs. 2 and 3), and their sequence analysis revealed that MtrA recognizes direct repeat motifs resembling GTCACAgcg (Fig. 4) and that binding affinity is increased by MtrA phosphorylation (Fig. 2 and supplemental Figs. S2–S4).

The accuracy of our proposed MtrA recognition sequences is further supported by comparison with the recognition sequences of related RR proteins. MtrA was originally identified by a strong hybridization with cloned PhoB DNA (6), and amino acids sequence alignments confirm a strong affiliation with the PhoB RR family (data not shown). *E. coli* PhoB RR plays a critical role in regulating the genes involved in the phosphate utilization pathway (5, 37, 38). Alignment of the published PhoB recognition sequences of *E. coli*, *Sinorhizobium meliloti* (39), and *Streptomyces coelicolor* (40) with our proposed MtrA recognition sequences, whose direct repeats are spaced for optimal MtrA binding (+2 spacing, see supplemental Fig. S5), revealed that all of these sequences share the common core GTCA direct repeats with an 11-bp helical repeat. This would place the recognition motifs on the same face of the B-form DNA helix, like other typical DNA-binding proteins.

Overall, most of our MtrA binding data is consistent with the standard model for PhoB and related response regulators, where phosphorylation stimulates dimer protein binding to two direct DNA repeats. This is how we interpreted MtrA binding at the individual *ori*C footprints, and this interpretation is easily extended to the *fbp*B promoter, where we propose that phosphorylation stimulates the binding of two MtrA dimers to four direct DNA repeats. It should be noted that the *fbp*B promoter direct repeats only partially match our proposed MtrA recognition sequences. However, this defect is presumably compensated by the optimal +2 spacing and perhaps by cooperative binding between four MtrA molecules (one per direct repeat). It is pertinent to recognize that although the *fbp*B genes of *Mtb* and other mycobacterial members are identified, detailed promoter analyses, including the identification of −35 and −10 elements, have not been reported. Nonetheless, analysis of the 175 bp upstream of different *fbp*B regions clearly shows significant sequence conservation under the MtrA footprint (see supplemental Fig. S7 for further details). Conservation of the sequences in the footprinted region of different mycobacterial species further supports our conclusion that the *fbp*B promoter is an MtrA target.

Although our results argue that MtrA recognizes GTCACA motifs with this typical 11-bp helical repeat, our results also unexpectedly argue for the usage of atypical 9- and 7-bp helical repeats (described as +2, 0, and −2 spacing between 9-bp direct repeats in Fig. 4). Presumably, MtrA binding to DNA is best when the 6-bp motif is on the same face of the helix. Using the F2 *ori*C as an example, we showed that MtrA binding to F2 requires the GTCACA motif, and it is barely detectable unless the natural spacing is increased from 0 to +2 or +3 (supplemental Fig. S4). Despite this intrinsically weak affinity for MtrA, three points argue that F2 is physiologically important and perhaps critical for replication control. First, changing only the GTCACA repeats in F2 abolished the autonomous replication activity of the *Mtb ori*C plasmid in *Mtb* (pMMR87, Fig. 6). Previous studies showed that mutations in DnaA-boxes comparably impaired the autonomous replication activity of *ori*C plasmids (9, 13, 33). Second, the atypically spaced GTCACA repeats in F2 are conserved among diverse *Mycobacteria* species (supplemental Fig. S4). Only DnaA-boxes show a comparable degree of conservation among these *ori*C DNA sequences. F2 is perfectly conserved among *Mtb*, *M. leprae,* and *Mycobacterium avium* (supplemental Fig. S6). Interestingly, in the more distant species, where base pair changes are seen in the corresponding GTCACA repeats, additional and perhaps compensatory GTCACA repeats are present. For example, *Mycobacterium smegmatis* and *Mycobacterium flavescens* have a third perfect GTCACA motif with the same atypical spacing. This observation further suggests a selective pressure for creating MtrA-binding sites and not simply the lack of genetic drift.

Third, F2 is located inside *ori*C, between the DnaA-boxes and the AT-rich unwinding site (supplemental Fig. S5) (41). Although detailed molecular details on how the initiation of DNA replication in *Mtb* occurs are unknown, recent studies reveal that the initial interactions of DnaA with DnaA-boxes in the presence of ATP are necessary for a rapid oligomerization of DnaA at *ori*C and the formation of the DnaA-*ori*C initiation complex competent for initiation (42). This initial step is followed by unwinding of *ori*C at the AT-rich sequences, which can occur in the absence of helicases and other replication proteins (41). Thus, the strategic location of F2 in *ori*C suggests that MtrA bound at F2 either aids or interferes with these key

replication steps (see below). Although detailed studies are required to understand the mechanism of action, results presented in Fig. 6 suggest that MtrA activity is necessary for maintaining stable autonomous replication of *ori*C plasmids. The relative weakness of the F2 MtrA-binding site argues that it is bound *in vivo* when the ratio of MtrA~P to MtrA is high.

The MtrA-*ori*C footprinting data show that MtrA at the 814-bp *ori*C region produces seven shorter (~30 bp) footprints (F1, F2, F3, F4, F5, F6A, and F6B) and several even shorter (~10 bp) points of DNase I protection that we called toe prints (Fig. 3). It should however be noted that the *dna*A-*dna*N intergenic region has just four MtrA-binding sites (see Fig. 3*C*: F2, F3, F4, and F5). Such dispersed contacts across all of *ori*C, including the *dnaA* 3′- and *dnaN* 5′-coding DNA, are more typical of DnaA protein binding to multiple DnaA-boxes that span bacterial *ori*Cs, including *Mtb ori*C (42). It is possible that the toe prints are not true MtrA-binding sites but rather could be due to the consequence of the formation of large MtrA-*ori*C nucleoprotein complexes. Presumably, these could be similar to the observed weaker DnaA-binding sites of *E. coli ori*C, which can be mutated without any effect (43). Further studies are required to address this issue. It is pertinent to note that in *E. coli* cells, DnaA persistently binds to the high affinity DnaA-boxes in *ori*C, but the key low affinity DnaA-boxes are unoccupied until they are required during the initiation of chromosome replication. This high to low affinity DnaA-box hierarchy is an important part of the *E. coli ori*C regulatory system (44). The *Caulobacter crescentus* response regulator CtrA binds five sites spread across its replication origin (45). Perhaps like the multiple DnaA-boxes, the multiple *ori*C MtrA-binding sites may form a hierarchy of persistently bound (high affinity) sites and transiently bound (low affinity such as F2) sites that are similarly required for *Mtb ori*C replication control. Clearly, further studies are required to address how MtrA controls *ori*C replication.

How might MtrA activity function to regulate *ori*C replication? The MtrA contact sites in *ori*C are distinctly different from the DnaA-boxes (42). This makes it unlikely that MtrA binding to *ori*C affects the first step of initiation, namely the binding of the DnaA protein to DnaA-boxes and vice versa. However, MtrA binding to *ori*C could either aid or hinder the ability of the DnaA protein to oligomerize at *ori*C and could thereby control the replication initiation process. Because MtrA~P preferentially binds to these targets, we propose that, under normal growth conditions where signals for MtrA phosphorylation are limiting and tightly regulated by the cognate MtrB sensor kinase, the MtrA-*ori*C interactions lead to regulated replication resulting in stable autonomous replication. Thus, the absence of MtrA-boxes as in pMMR87 and pMMR88 (see Fig. 6) could impair *ori*C plasmid replication possibly leading to plasmid loss. However, for growth conditions that promote an elevated MtrA~P state, *i.e.* during intracellular growth in cells overproducing MtrA in the absence of MtrB, it is expected that the elevated pools of MtrA~P can access all of its recognition sequences in *ori*C. This situation could lead to an interference with the DnaA protein binding to *ori*C and the formation of the *ori*C-DnaA initiation complex. This line of thinking leads us to speculate that MtrA can play a positive or a negative role depending upon its phosphorylation potential. Perhaps the elevated pools of MtrA~P limits the ability of the DnaA protein to initiate replication during nonreplicative persistence or the chronic stage of infection.

One unexpected finding is that the pMQ219 plasmid, which replicates extrachromosomally in the WT background, is excluded in WT cells carrying integrated plasmid vector, *i.e.* Rv19. This result is independent of MtrA overproduction phenotypes (see supplemental Fig. S6 and legend). The mycobacterial shuttle vectors based on pAL5000 replication origin (34) generally replicate as free plasmids in the integrated plasmid background. The pMQ219, which is a derivative of pZErO 2.1 plasmid (9), and the integration plasmid pJFr-19, which is used to affect MtrA levels (8), share more than the 800-bp region of homology. It is possible that some factors or components involved in *Mtb ori*C replication function in recombination; these mechanisms are not yet fully understood. Although speculative, such factors, if any, could preferentially promote recombination between pMQ219 and the resident plasmid at the region of homology resulting in integration events when both *ori*C sequences are primed for initiation. Further studies, including the construction and characterization of minichromosomes lacking such homologous sequences, are required to understand why the pMQ219 plasmid is excluded in the Rv19 background.

Although detailed studies are required to understand the roles of MtrA on *ori*C replication, stability experiments revealed that optimal levels of MtrA, irrespective of its phosphorylation state, are required for the maintenance of integrated *ori*C plasmid sequences in Rv78 and Rv129 backgrounds (Fig. 7). We envision that MtrA influences *ori*C replication, and hence under overproduction conditions promote activation of *ori*C at the integrated locus. This could then potentially create *ori*C incompatibility issues as the presence of activated *ori*C at two different regions on the chromosome, *i.e.* native as well as integrated locus, could be detrimental for normal cell cycle progression (36). A consequence is the loss of plasmid-bearing *ori*C sequences. One intriguing finding of our data is that, unlike the WT Rv19 cells, the integrated *ori*C plasmids are not stably maintained in merodiploids overproducing phosphorylation-defective *Mtb*(D53N, MtrA$^+$) MtrA protein. It should be noted that our experiments were carried out with MtrA merodiploid strains but not with the strains producing phosphorylation-defective *Mtb*(D53N, MtrA$^+$) as the sole source. Thus, it is likely the *Mtb*(D53N, MtrA$^+$) will have both homo- and heterodimers of MtrA, and both species could be competent in affecting *ori*C replication. Future studies with *Mtb mtr*A mutants producing MtrA(D53N) as the sole source for MtrA will be required to address these issues.

In contrast to *ori*C, MtrA at the *fbp*B promoter produced one discrete long (~60 bp) footprint (Fig. 2), consistent with four MtrA molecules binding together. This binding clearly shows a preference for MtrA~P (Fig. 2*A*). Evaluation of the binding characteristics of MtrA to the *fbp*B promoter and *ori*C may reflect different regulatory functions. For example, MtrA makes one focused contact inside the *fbp*B promoter, as is typical of transcriptional regulators. This argues that MtrA~P acts as a transcriptional repressor for the *fbp*B gene. Such transcriptional repression could occur under the conditions that elevate the MtrA phosphorylation state. Earlier studies revealed that

the phosphorylation potential of MtrA is elevated during intramacrophage growth in cells overproducing phosphorylation-competent MtrA in the absence of the MtrB sensor kinase (8). *Mtb* secretes copious amounts of highly immunogenic Ag85B protein (46), whose processed peptides contain epitopes for T-cell recognition (35). Thus, the reduced expression of *fbp*B upon infection under elevated MtrA~P conditions could limit the available pools of secreted antigen 85B for its subsequent processing by antigen presentation pathways. It is pertinent to note that the MtrA footprinted region of *fbp*B promoter is well conserved in other mycobacterial species as well (see supplemental Fig. S7).

Interestingly, analysis of *fbp*A expression under MtrA overproduction conditions, however, revealed a different expression profile from that of *fbp*B (supplemental Fig. S8). The expression of *fbp*A was reduced in Rv19 *Mtb* WT cells upon macrophage infection, although it was elevated in both Rv78 *Mtb*(MtrA$^+$) and Rv129 *mtrA* merodiploids (supplemental Fig. S8). The phosphorylation-independent increase in the *fbp*A expression in Rv129 *Mtb* (D53N MtrA$^+$) merodiploid suggests that the regulation of *fbp*A is different and not directly dependent on a balanced amount of MtrA phosphorylation. Also, because the ChIP signal for *Pfbp*A is weaker than for *pfbp*B (Fig. 1), it is possible that the observed changes in the *fbp*A expression are due to secondary effects or to more distant binding sites. It is unknown if expression of genes responsible for other secreted antigens and other immunodominant proteins are also affected by MtrA. Nonetheless, MtrA~P-dependent reduction of the expression of *fbp*B and possibly other unrecognized genes responsible for antigenic proteins could be one of the many immune evasion mechanisms the pathogen uses for its long term persistent growth during chronic infection and in granuloma.

Acknowledgments—We thank Naveen Nair for technical assistance, Dr. A. Chauhan and Erin Maloney for RNA preparation and Southern experiments, Meredith Moomey for help with the construction of oriC plasmids, and Dr. Julia Grimwade for helpful advice and carrying out preliminary footprinting experiments.

REFERENCES

1. North, R. J., and Jung, Y. J. (2004) *Annu. Rev. Immunol.* **22,** 599–623
2. Kaufmann, S. H., Cole, S. T., Mizrahi, V., Rubin, E., and Nathan, C. (2005) *J. Exp. Med.* **201,** 1693–1697
3. Smith, I. (2003) *Clin. Microbiol. Rev.* **16,** 463–496
4. Cole, S. T., Brosch, R., Parkhill, J., Garnier, T., Churcher, C., Harris, D., Gordon, S. V., Eiglmeier, K., Gas, S., Barry, C. E., 3rd, Tekaia, F., Badcock, K., Basham, D., Brown, D., Chillingworth, T., Connor, R., Davies, R., Devlin, K., Feltwell, T., Gentles, S., Hamlin, N., Holroyd, S., Hornsby, T., Jagels, K., Krogh, A., McLean, J., Moule, S., Murphy, L., Oliver, K., Osborne, J., Quail, M. A., Rajandream, M. A., Rogers, J., Rutter, S., Seeger, K., Skelton, J., Squares, R., Squares, S., Sulston, J. E., Taylor, K., Whitehead, S., and Barrell, B. G. (1998) *Nature* **393,** 537–544
5. Hoch, J. A. (2000) *Curr. Opin. Microbiol.* **3,** 165–170
6. Via, L. E., Curcic, R., Mudd, M. H., Dhandayuthapani, S., Ulmer, R. J., and Deretic, V. (1996) *J. Bacteriol.* **178,** 3314–3321
7. Zahrt, T. C., and Deretic, V. (2000) *J. Bacteriol.* **182,** 3832–3838
8. Fol, M., Chauhan, A., Nair, N. K., Maloney, E., Moomey, M., Jagannath, C., Madiraju, M. V., and Rajagopalan, M. (2006) *Mol. Microbiol.* **60,** 643–657
9. Qin, M. H., Madiraju, M. V., and Rajagopalan, M. (1999) *Gene* **233,** 121–130
10. Chauhan, A., Madiraju, M. V., Fol, M., Lofton, H., Maloney, E., Reynolds, R., and Rajagopalan, M. (2006) *J. Bacteriol.* **188,** 1856–1865
11. Rajagopalan, M., Atkinson, M. A., Lofton, H., Chauhan, A., and Madiraju, M. V. (2005) *Biochem. Biophys. Res. Commun.* **331,** 1171–1177
12. Yamamoto, K., Low, B., Rutherford, S. A., Rajagopalan, M., and Madiraju, M. V. (2001) *Biochem. Biophys. Res. Commun.* **280,** 898–903
13. Qin, M. H., Madiraju, M. V., Zachariah, S., and Rajagopalan, M. (1997) *J. Bacteriol.* **179,** 6311–6317
14. Siam, R., Brassinga, A. K., and Marczynski, G. T. (2003) *J. Bacteriol.* **185,** 5563–5572
15. Abou-Zeid, C., Garbe, T., Lathigra, R., Wiker, H. G., Harboe, M., Rook, G. A., and Young, D. B. (1991) *Infect. Immun.* **59,** 2712–2718
16. Content, J., de la Cuvellerie, A., De Wit, L., Vincent-Levy-Frébault, V., Ooms, J., and De Bruyn, J. (1991) *Infect. Immun.* **59,** 3205–3212
17. Wiker, H. G., and Harboe, M. (1992) *Microbiol. Rev.* **56,** 648–661
18. Belisle, J. T., Vissa, V. D., Sievert, T., Takayama, K., Brennan, P. J., and Besra, G. S. (1997) *Science* **276,** 1420–1422
19. Brennan, P. J., and Nikaido, H. (1995) *Annu. Rev. Biochem.* **64,** 29–63
20. Goren, M. B. (1972) *Bacteriol. Rev.* **36,** 33–64
21. Wilkinson, R. J., DesJardin, L. E., Islam, N., Gibson, B. M., Kanost, R. A., Wilkinson, K. A., Poelman, D., Eisenach, K. D., and Toossi, Z. (2001) *Mol. Microbiol.* **39,** 813–821
22. Pai, S. R., Actor, J. K., Sepulveda, E., Hunter, R. L., Jr., and Jagannath, C. (2000) *Microb. Pathog.* **28,** 335–342
23. Shi, L., Jung, Y. J., Tyagi, S., Gennaro, M. L., and North, R. J. (2003) *Proc. Natl. Acad. Sci. U.S.A.* **100,** 241–246
24. Shi, L., North, R., and Gennaro, M. L. (2004) *Infect. Immun.* **72,** 2420–2424
25. Bramhill, D., and Kornberg, A. (1988) *Cell* **54,** 915–918
26. Bramhill, D., and Kornberg, A. (1988) *Cell* **52,** 743–755
27. Zyskind, J. W., and Smith, D. W. (1986) *Cell* **46,** 489–490
28. Casali, N., White, A. M., and Riley, L. W. (2006) *J. Bacteriol.* **188,** 441–449
29. Chauhan, A., Lofton, H., Maloney, E., Moore, J., Fol, M., Madiraju, M. V., and Rajagopalan, M. (2006) *Mol. Microbiol.* **62,** 132–147
30. Shimono, N., Morici, L., Casali, N., Cantrell, S., Sidders, B., Ehrt, S., and Riley, L. W. (2003) *Proc. Natl. Acad. Sci. U.S.A.* **100,** 15918–15923
31. Haydel, S. E., and Clark-Curtiss, J. E. (2004) *FEMS Microbiol. Lett.* **236,** 341–347
32. Rajagopalan, M., Qin, M. H., Nash, D. R., and Madiraju, M. V. (1995) *J. Bacteriol.* **177,** 6527–6535
33. Dziadek, J., Rajagopalan, M., Parish, T., Kurepina, N., Greendyke, R., Kreiswirth, B. N., and Madiraju, M. V. (2002) *J. Bacteriol.* **184,** 3848–3855
34. Kana, B. D., and Mizrahi, V. (2004) *Tuberculosis* **84,** 63–75
35. Mustafa, A. S., Shaban, F. A., Abal, A. T., Al-Attiyah, R., Wiker, H. G., Lundin, K. E., Oftung, F., and Huygen, K. (2000) *Infect. Immun.* **68,** 3933–3940
36. Dasgupta, S., and Løbner-Olesen, A. (2004) *Plasmid* **52,** 151–168
37. Blanco, A. G., Sola, M., Gomis-Rüth, F. X., and Coll, M. (2002) *Structure* **10,** 701–713
38. Zundel, C. J., Capener, D. C., and McCleary, W. R. (1998) *FEBS Lett.* **441,** 242–246
39. Yuan, Z. C., Zaheer, R., Morton, R., and Finan, T. M. (2006) *Nucleic Acids Res.* **34,** 2686–2697
40. Sola-Landa, A., Rodríguez-García, A., Apel, A. K., and Martín, J. F. (2008) *Nucleic Acids Res.* **36,** 1358–1368
41. Farhana, A., Kumar, S., Rathore, S. S., Ghosh, P. C., Ehtesham, N. Z., Tyagi, A. K., and Hasnain, S. E. (2008) *PLoS ONE* **3,** e2087
42. Madiraju, M. V., Moomey, M., Neuenschwander, P. F., Muniruzzaman, S., Yamamoto, K., Grimwade, J. E., and Rajagopalan, M. (2006) *Mol. Microbiol.* **59,** 1876–1890
43. Riber, L., Fujimitsu, K., Katayama, T., and Løbner-Olesen, A. (2009) *Mol. Microbiol.* **71,** 107–122
44. Leonard, A. C., and Grimwade, J. E. (2005) *Mol. Microbiol.* **55,** 978–985
45. Siam, R., and Marczynski, G. T. (2000) *EMBO J.* **19,** 1138–1147
46. Harth, G., Horwitz, M. A., Tabatadze, D., and Zamecnik, P. C. (2002) *Proc. Natl. Acad. Sci. U.S.A.* **99,** 15614–15619